SMART DIASPORA 2023

Prevention, diagnostic and personalized treatment in solid tumors

Focus on tumor microenvironment

Assoc. Prof. Florina Bojin, MD, PhD

UMF “Victor Babeș” Timișoara, Department III - Functional Sciences
SCJU “Pius Brînzeu” Timișoara, OncoGen Centre

Project:
Tumor-associated fibroblasts as novel target in anti-tumor therapy – identification of origin, role and characteristic molecular markers, PNII-Idei No. 318/2011 (2012-2016)

Characterization of tumor-associated fibroblasts (TAFs) in 2D culture

The tumor microenvironment

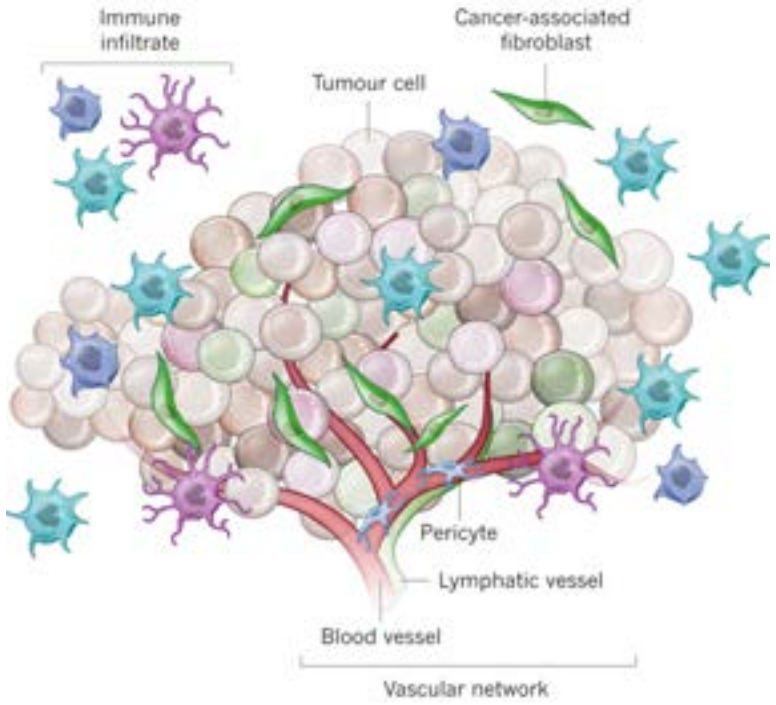

- Tumor microenvironment (TME) is created by the interaction between malignant cancer cells and non-transformed cells
- The structural and functional elements of the tumor stroma: immune cells, vasculature, TAFs
- Cancer cells convert the TME into a pathologically active niche that guides tumor progression

- Isolation of TAFs from solid tumours
- Morphologic characterization – electron microscopy
- Immunophenotypic assessment of TAFs – ICC, IF, Flow
- Multipotent / Pluripotent ability – differentiation studies
- Functional abilities of TAFs to support tumor development – flowchamber, ELISA

Morphologic characterization of TAFs

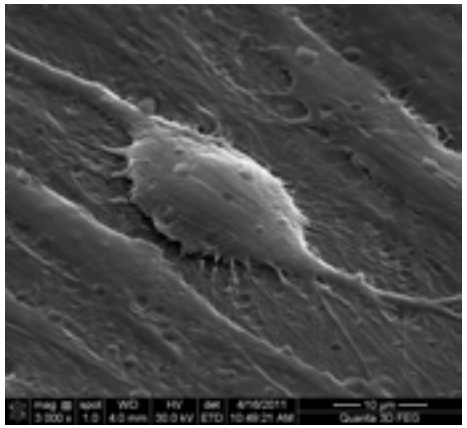

MSC

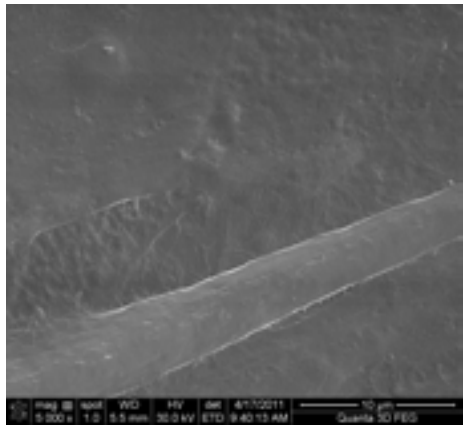

TAF

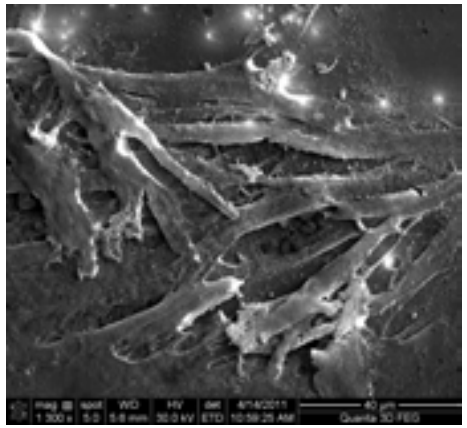

DSC

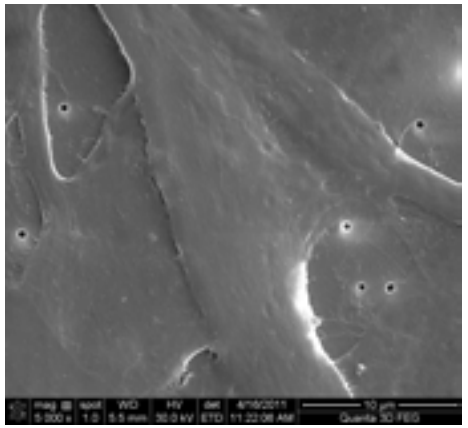

MuSC

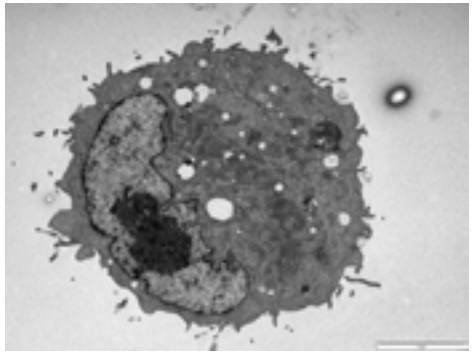

Phyllopoda/lamellipodia

Ø = 15-20 µm

Zigzag ribosomes

Dense, dark mitochondria

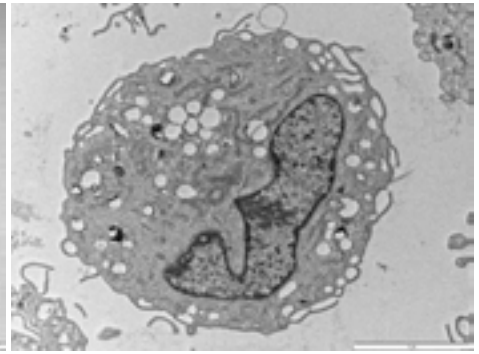

Phyllopoda/lamellipodia

Ø = 20-25 µm

Zigzag ribosomes

Organized fibers, vesicles

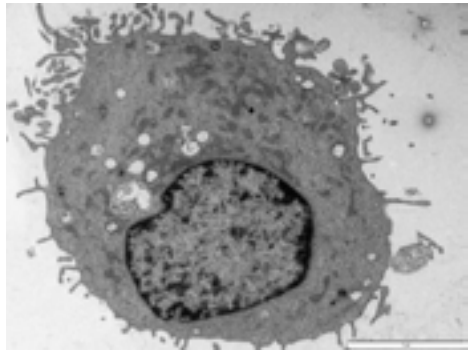

Phyllopoda/lamellipodia

Ø = 15 µm

Zigzag ribosomes

Polyribosomes

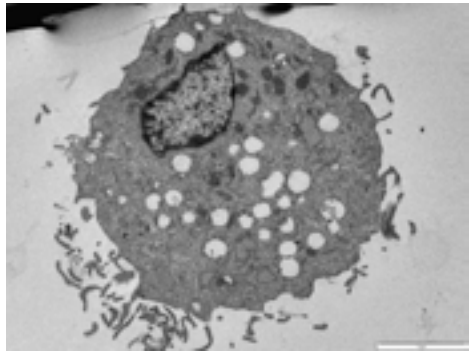

Phyllopoda/lamellipodia

Ø = 25-30 µm

Zigzag ribosomes

Dilated cistern

Immunophenotypic analysis of stem cells with different tissue origins

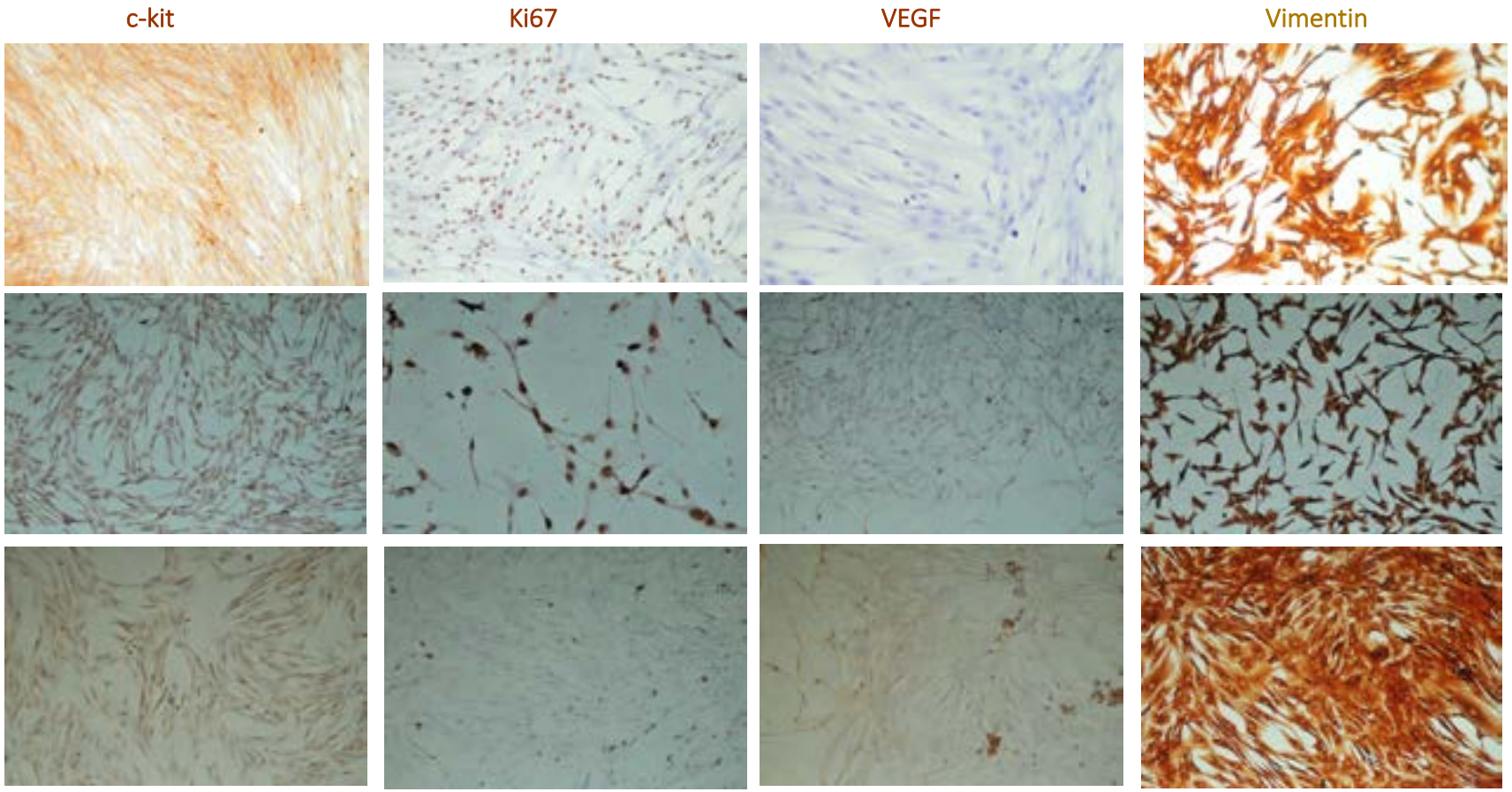

- UCSC - the highest proliferation rate, Ki67 presence in approximately 80% cells
- VEGF was present in 20-30% of initial MuSC cells, absent in other stem cells
- Cytoskeleton revealed by Vimentin presence in all cellular types
- CD117/c-kit present in various proportions in all cellular types (10-50%)

Immunophenotypic analysis of stem cells with different tissue origins

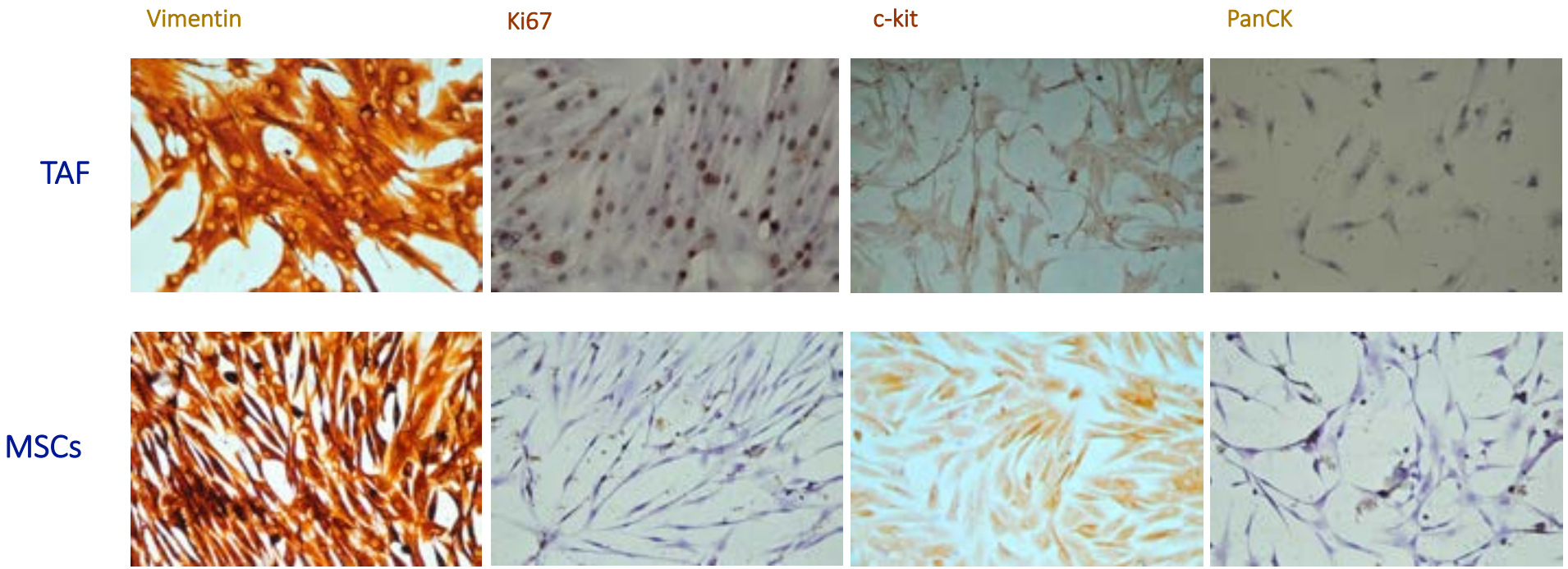

- Absence of Cytokeratin marker in MSC and TAF, cells being positive for Vimentin
- High proliferation rate of TAF (Ki67)
- CD117/c-kit (stem cell factor receptor) present in MSC and TAF → TAF are “MSC subset”

Differentiation studies – multipotent ability of stem cells

MSCs | TAFs | MuSCs

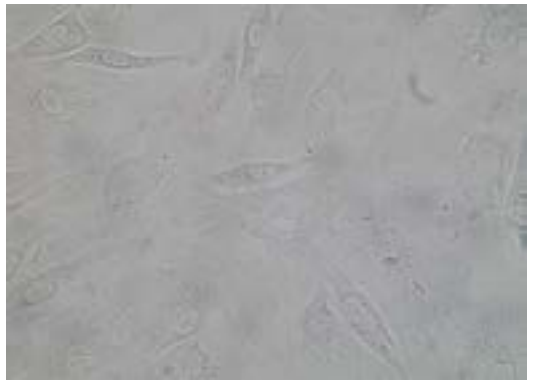

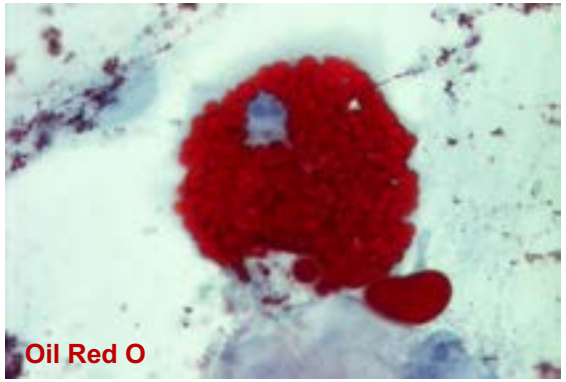

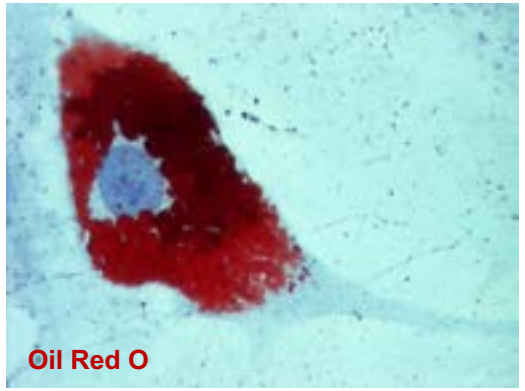

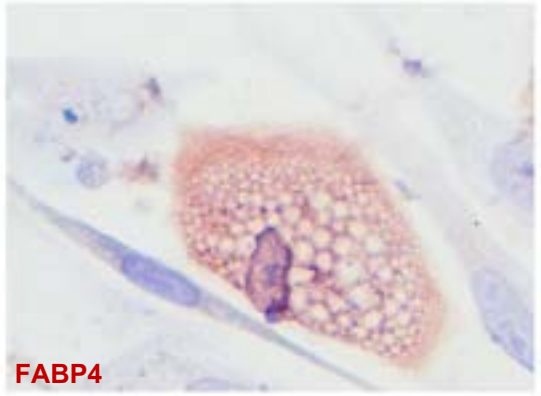

Adipocytic differentiation

- Only MSCs, TAFs and MuSCs were able to differentiate towards adipocytic lineage in appropriate media;
- MuSCs readily differentiated after 10 days, 70-80% of the cells being transformed into adipocytes.

Differentiation studies – multipotent ability of stem cells

Osteogenic and chondrocytic differentiation

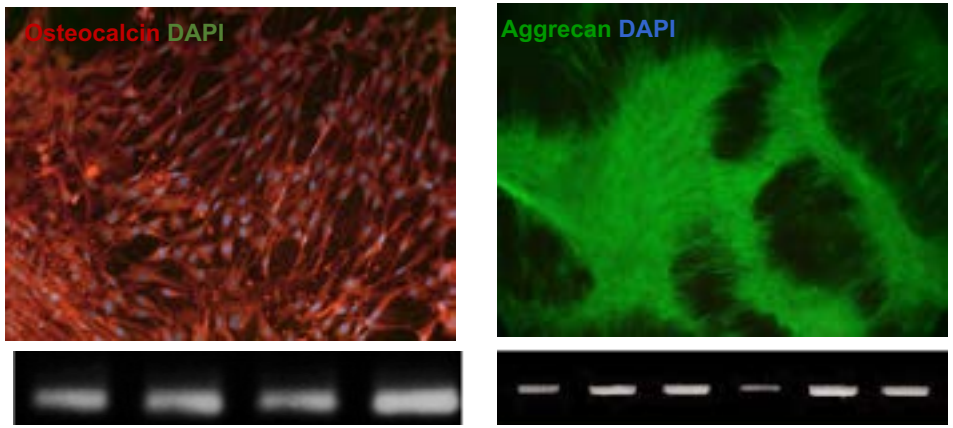

- MSC and TAF differentiated towards chondrocytic (presence of Aggrecan) and osteoblastic (positive staining for Osteocalcin) lineage
- DSC and MuSC were able to differentiate into mineralized cells and chondrocytes
- UCSC did not stain positive for any of the trilineage potential markers, but showed similar gene expression, thus suggesting their developmental immaturity

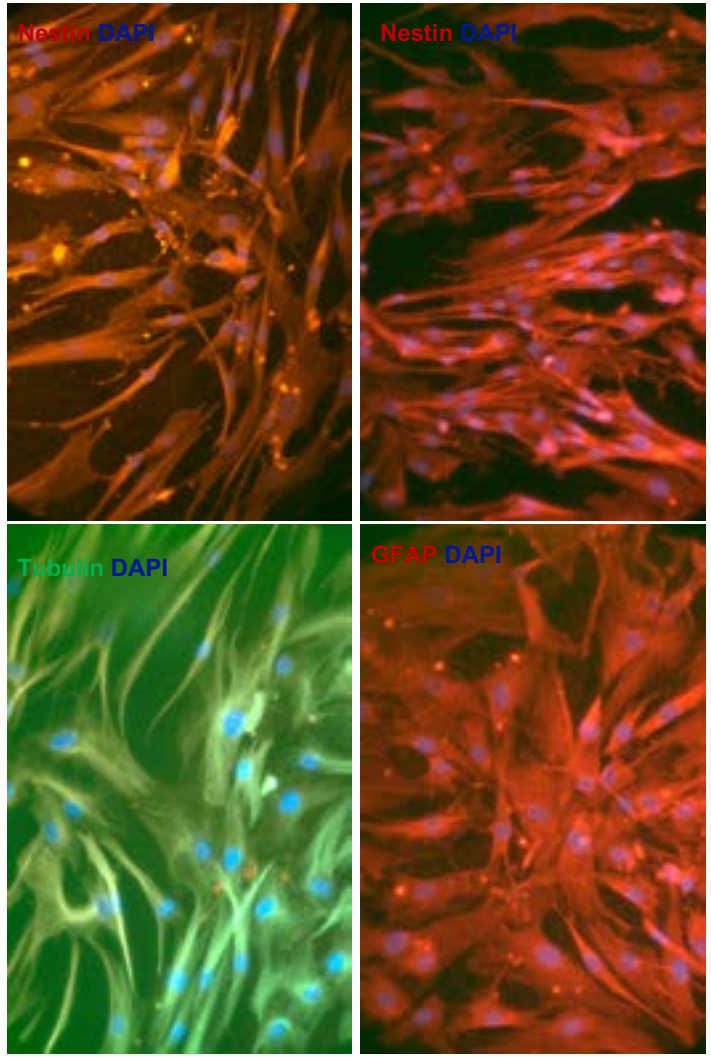

Neural-like cells differentiation

Differentiation studies – pluripotent ability

qRT-PCR stem cells

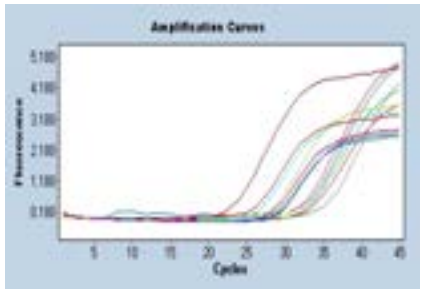

TAF

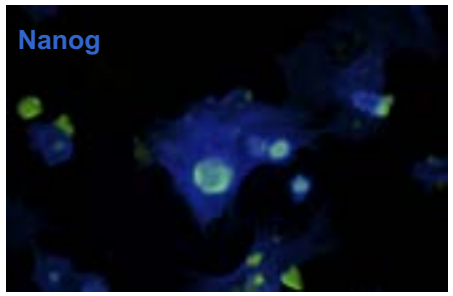

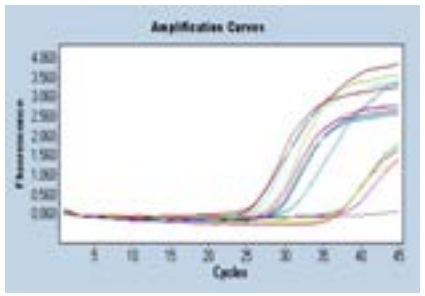

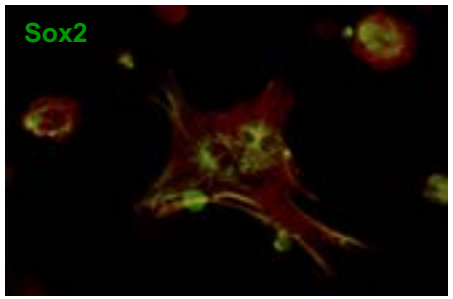

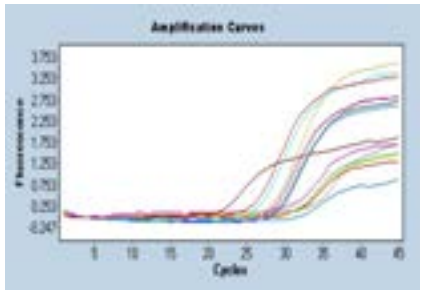

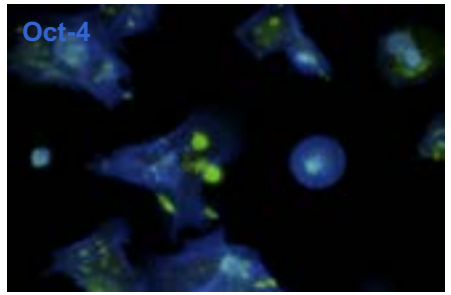

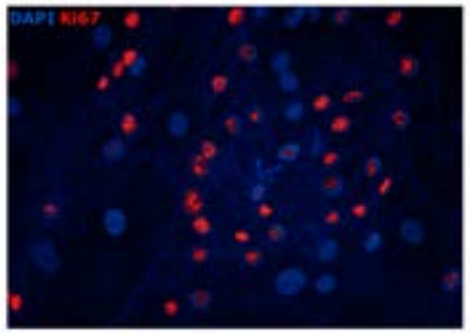

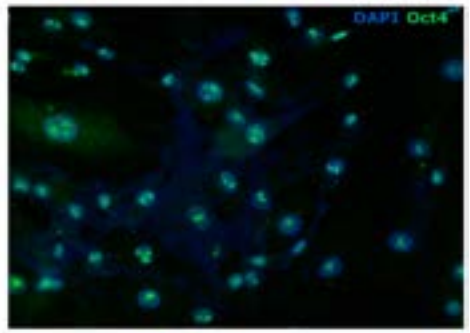

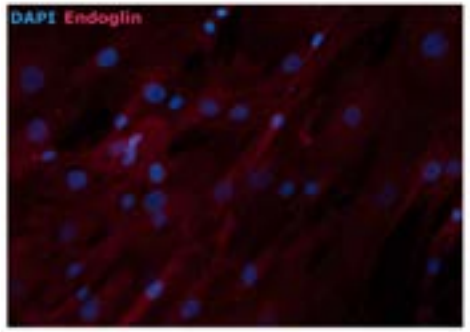

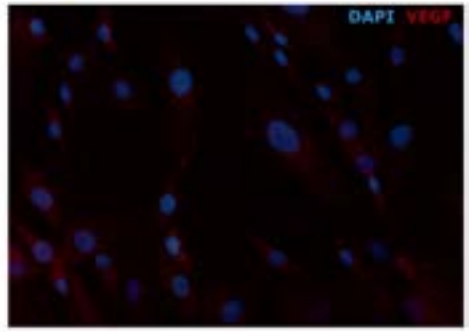

- TAFs showed the highest expression level of pluripotency - associated genes: Nanog, Sox2, Oct4
- Functional protein level was revealed only for TAFs and CD117/c-kit separated MuSC

Functional Studies – Flowchamber adhesion assay

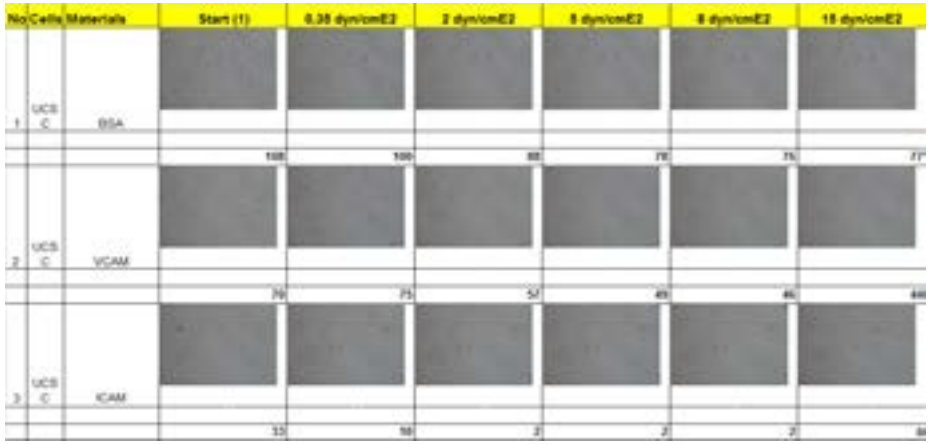

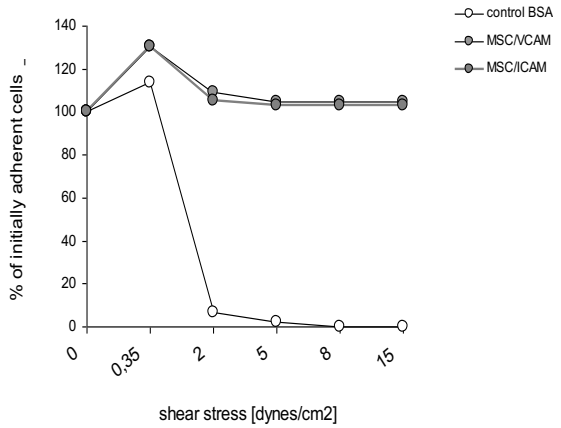

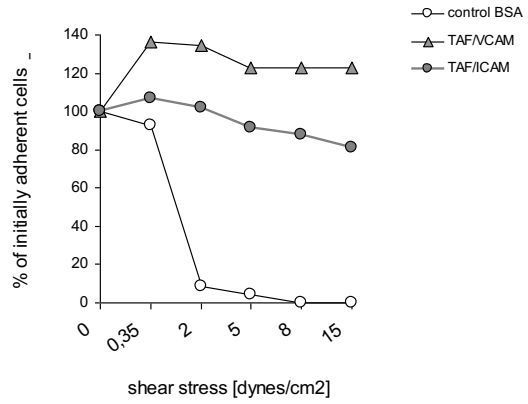

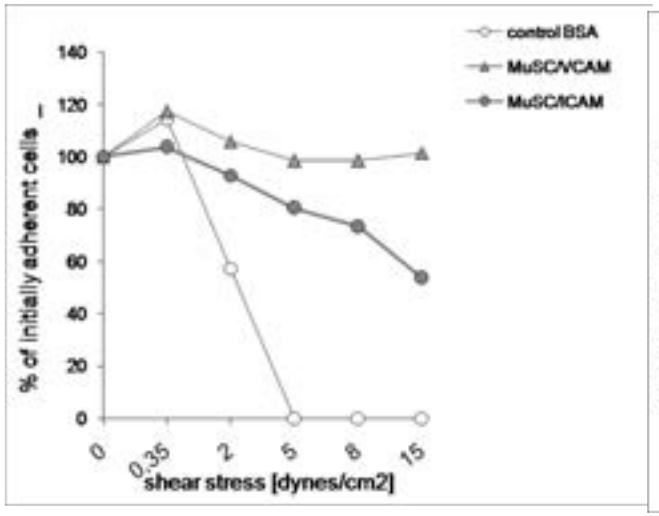

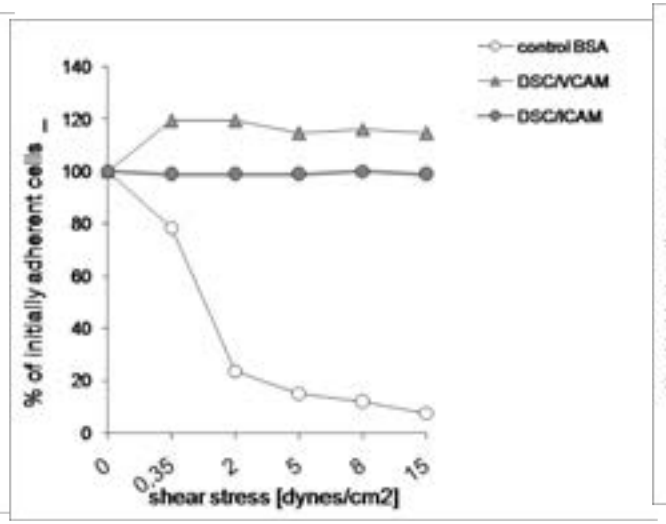

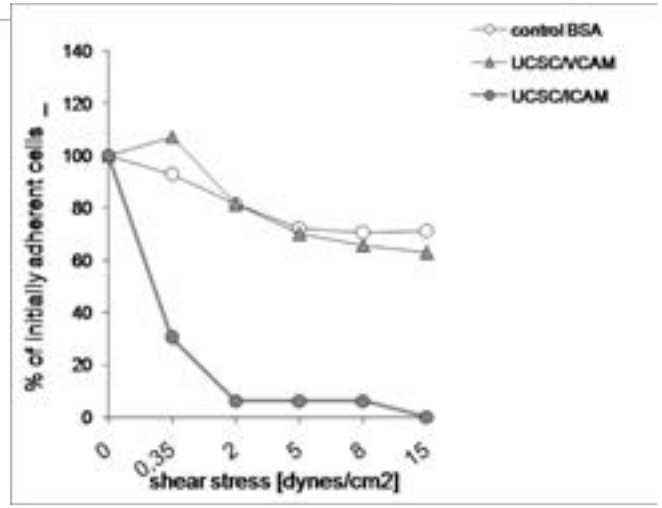

- Flowchamber channels coated with adhesion molecules (VCAM and ICAM) 0.2 mg/ml, at room temperature for 30 minutes
- 100,000 cells/channel are left to adhere for 3 minutes, than shear stress increase from 0.35 to 15 dyne/cm^2 is applied

Conclusion for *in vitro* characterization of TAFs

	MSCs	TAFs
Multipotency (trilineage differentiation potential)	yes	yes
Pluripotency capacity (Oct4, Sox2, Nanog)	no	yes
CD14, CD31, CD34, CD45, HLA-DR, CXCR4, VEGF-R1 (Flt-1), VEGF-R2 (Kdr), TGF-β RII	-	-
CD29, CD44, CD73, CD90, CD106, CD117	+	+
Cytoskeleton and extracellular matrix proteins		
Vimentin, α-SMA, Nestin	+	+
Cytokeratin, E-cadherin	-	-
Ultrastructural details		
Cytoplasmic elongations	no	yes
Lamellar content lysosoms	no	yes
Intermediate filaments	yes	no
Cytokines, chemokines and growth factors secretion		
IL-4, IL-10, IL-13, TGF-β1, TNF-α, VEGF	low	high

Paunescu V, *et al*. Tumor-associated fibroblasts and mesenchymal stem cells: more similarities than differences. *J Cell Mol Med*., 2011.

3D Models of Tumor Microenvironment

Project:
3D Bioprinting techniques for obtaining tissue constructs that mimic tumor microenvironment (DeLIMIT) 100PED/2017 (2017-2018)

Project:
Dezvoltarea de pachete software pentru biotipărirea tridimensională a modelelor tumorale pentru cercetări oncologice și validarea experimentală a acestora POSTDOC/1310/31.01.2020 (2020-2022)

Obtaining 3D structures that mimic the tumor microenvironment

- tumor models were fabricated by printing a hydrogel droplet (CELLINK, Sweden) of about 0.6 mm in diameter, employing a dedicated 3D printing software
- these tumor models with SK-BR3 breast cancer cells suspended in a concentration of 10^7 cells/ml were embedded in a hydrogel of the same type, loaded with primary cells isolated from the peritumoral environment (mostly made of tumor associated fibroblasts - TAFs and cells of the immune system - PBMCs).
- the bioprinted construct was subsequently immersed in Crosslinking Agent (CELLINK, Sweden) and exposed it to ultraviolet (365 nm) light for 2 minutes

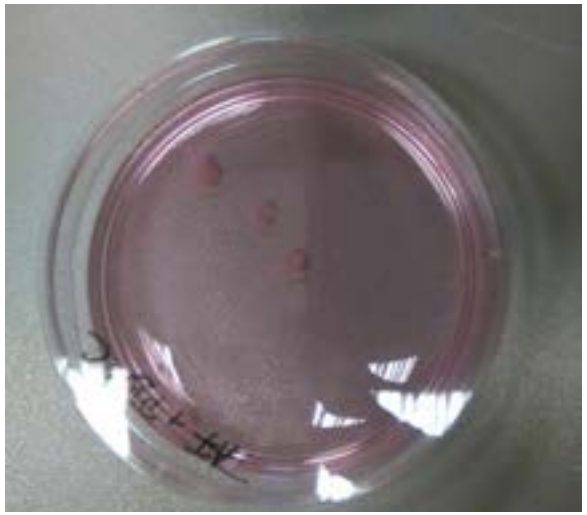

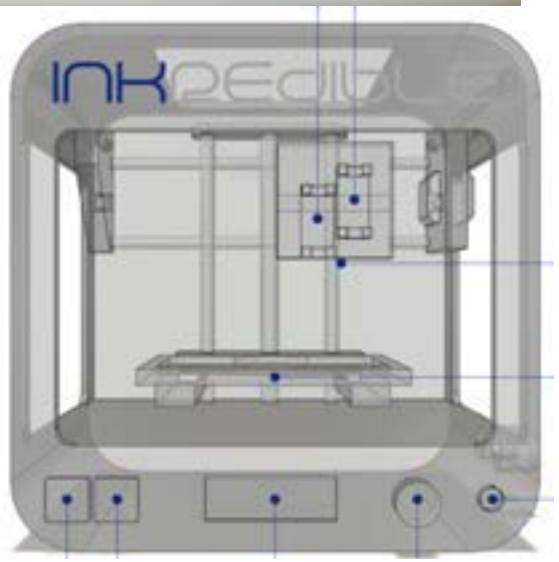

Computational model of 3D tumors

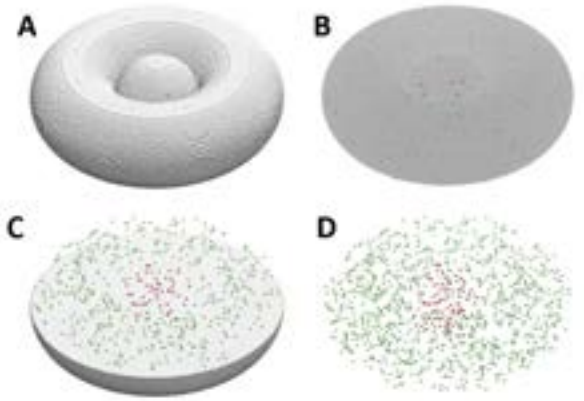

Computational model of toroidal tissue structure – perspective and lateral view (Visual Molecular Dynamics software – VMD, **Humphrey *et al.*, 1996**) tumor cells are represented by red dots, peri-tumoral cells are represented by green dots; hydrogel volume elements are represented by white spheres

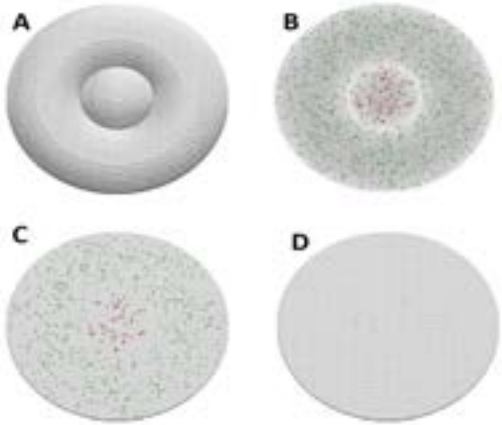

Computational model of toroidal tissue structure – external view.

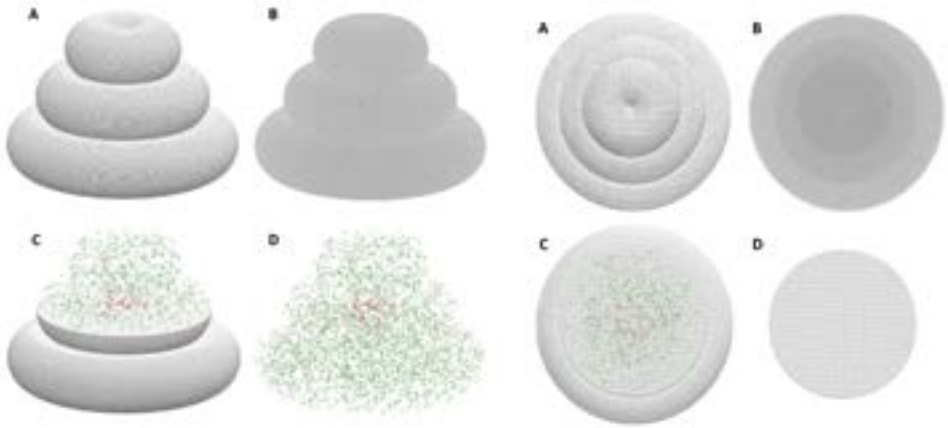

Computational model of triple-layer tissue structure – perspective and lateral view

Axial view of the triple-layered tissue structure

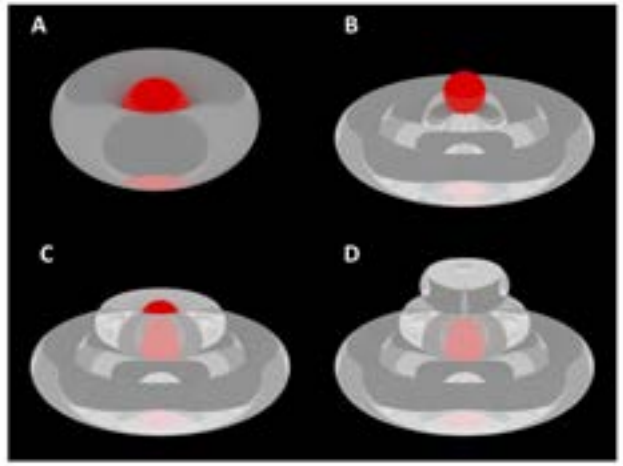

Bojin F., *et al.* Bioprinting of Model Tissue that Mimic the Tumor Microenvironment. *Micromachines*, 2021; 12: 535.

Computational model of 3D tumors – *in silico* evolution

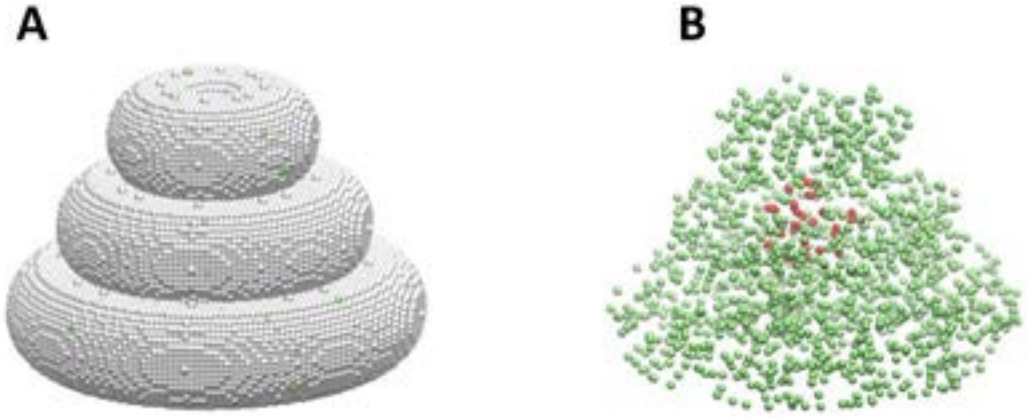

Initial configuration of triple-layered structure (1:3 scale) – lateral view (red = tumor cells, green = TAFs, white = hydrogel)

- In the computational study of the bioprinted constructs, we built 3D lattice models and simulated their evolution using the **Metropolis Monte Carlo** method

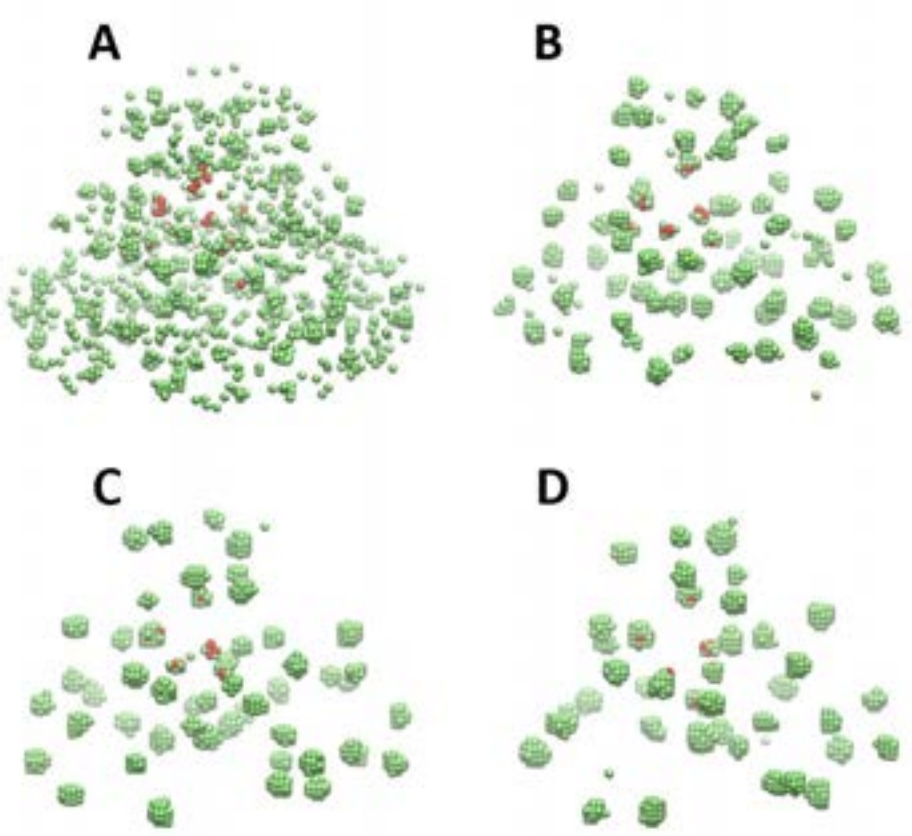

Evolution of 3D structure simulated using the SIMMMC software. **A-D** configurations obtained after running 10^2 MCS (**A**), 10^3 MCS (**B**), 10^4 MCS (**C**) and 5×10^4 MCS (**D**); the hydrogel is excluded for showing cellular relocation according to MMC algorithm

3D bioprinted structures – *in vitro* studies

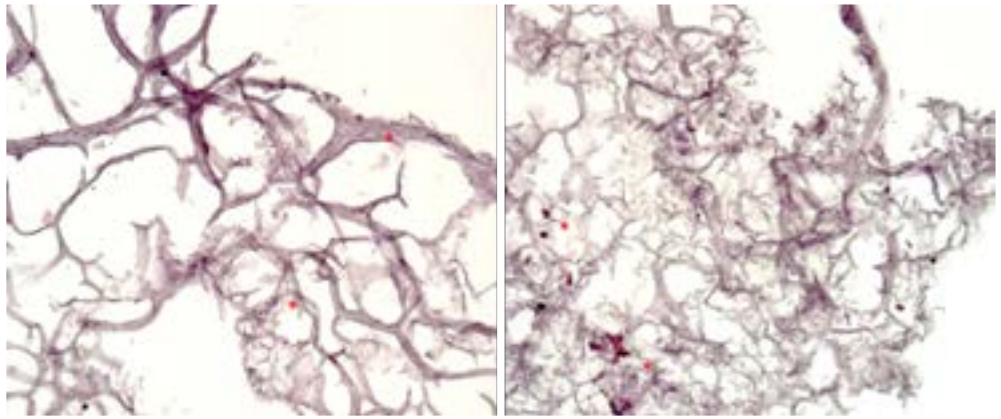

Histological analysis of representative sections of a triple-layered tissue construct

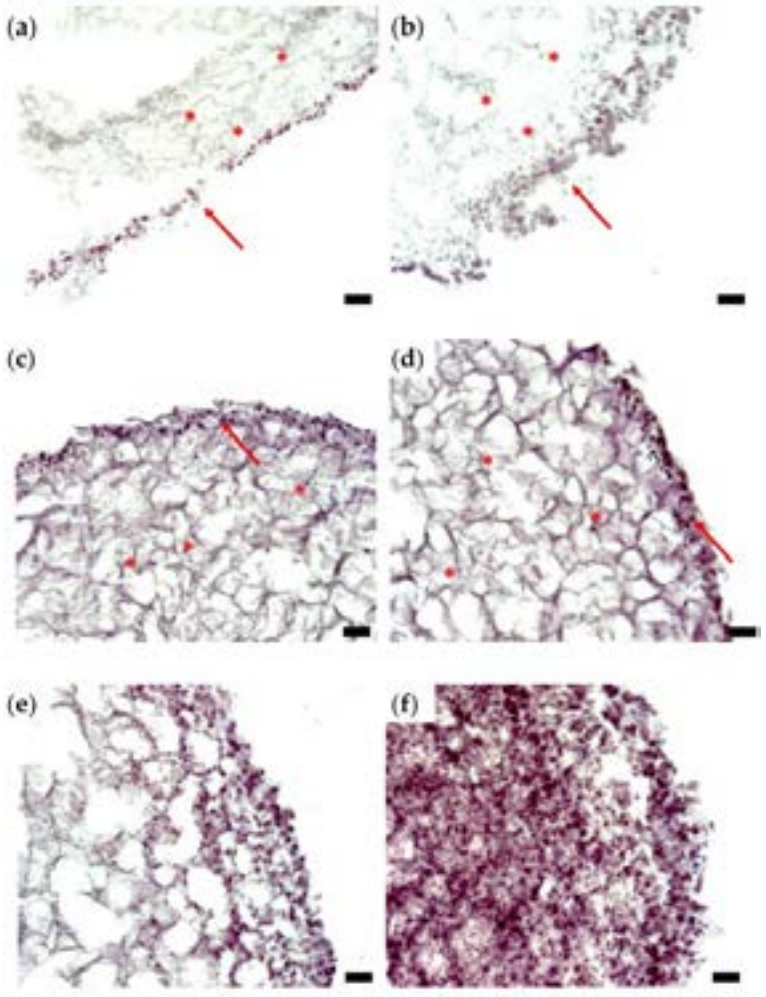

- *In vitro* tumor evolution is similar to *in vivo*-observed cellular arrangement
- The peripheral part of the tumor model is tempting a capsular structure, formed of monolayered cells alignment (D6), then stratified, ordered cellular arrangement (D14)
- Interior part of the tumoral model is represented by a network of bioprinting hydrogel, with tumor cells within the lattice
- Tumor model is fully developed after 14 days of *in vitro* culture in specific culture medium.

3D Bioprinted structures – *in vivo* studies

- the tissue models were cultured *in vitro* for 2 days, then implanted in CD1 Nu/Nu immunosuppressed mice (2 constructs per animal, inserted subcutaneously in the dorsal region, symmetrically with respect to the vertebral column)
- the constructs were retrieved after 8 weeks and evaluated histologically.

In vivo tumor evolution

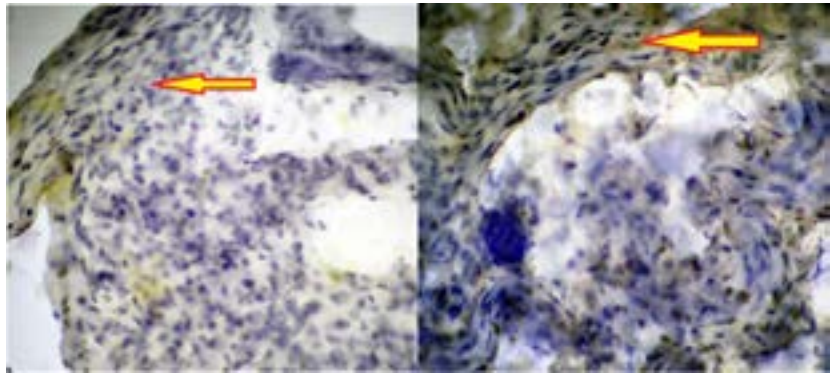

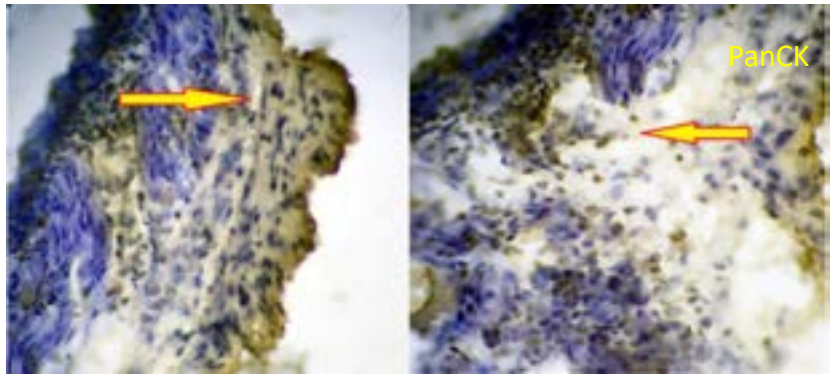

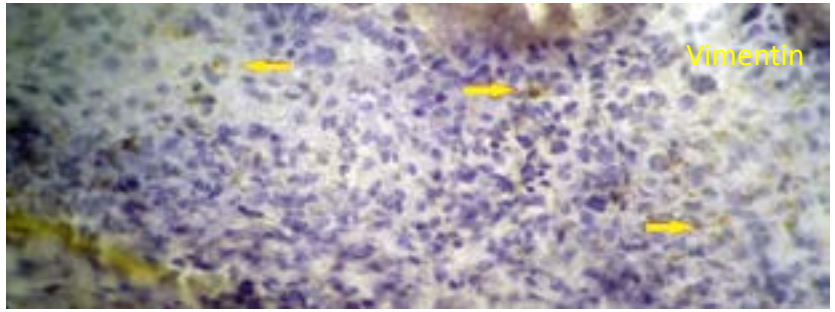

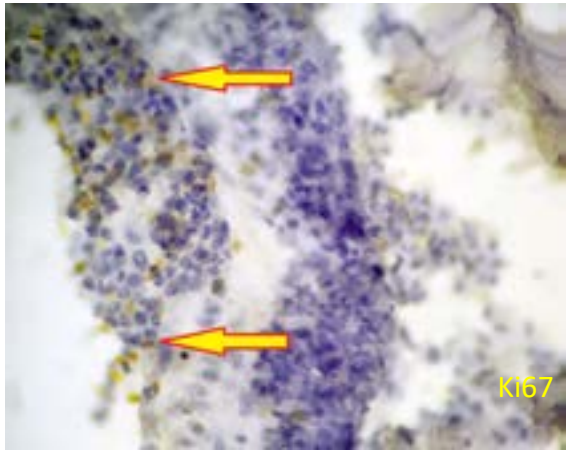

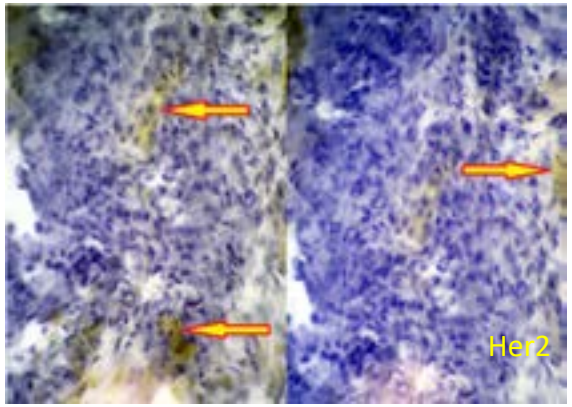

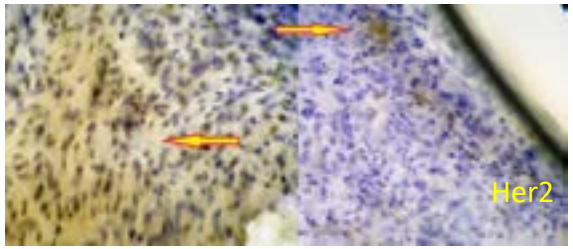

- After IHC staining and microscopic evaluation of ex vivo tumors we observed a good cellular development, with a slightly polymorphic distribution
- Small cellular size
- Two nuclei types: elongated, with condensed nuclear material, mainly at the periphery, tempting capsule formation; round-oval shape, with lax nuclear material, mostly distributed in the central part of the tumor

Long term in vivo tumor evolution


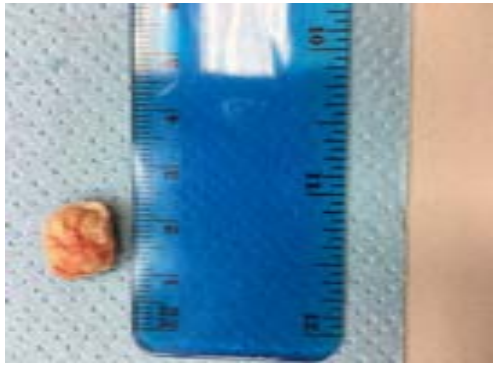


Macroscopic aspect of the tumor surgically removed from the mouse model CD1 Nu/Nu. Large tegument defect after tumors excision, the tumor being adherent only to the superjacent tissues (skin)

- 28 weeks of in vivo tumor development induced a dramatic increase of tumor size (5x, 1.5 cm), generation of abundant blood vessels and specific tumor capsule

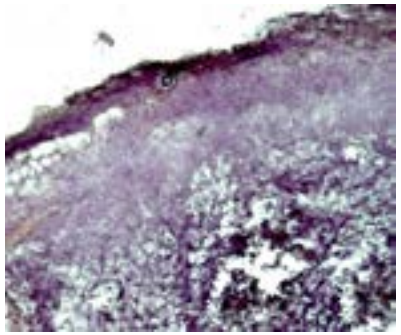
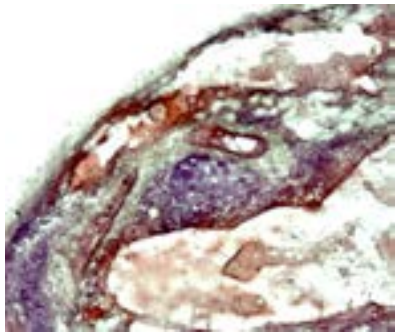
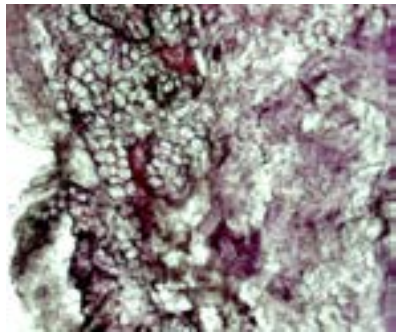

Histopathological aspect (HE staining) of the tumor surgically removed from the mouse model 28 weeks after implantation. The tumor is well organized: exterior capsule, numerous permeable blood vessels, and adipose tissue with lipid vacuoles (Ob. 10x)

3D Models of tumor microenvironment - Awards

Project:
Chimeric Antigen Receptor Targeted Oncoimmunotherapy with Natural Killer Cells (CAR-NK), SMIS code 103662 (2016-2020)

CAR Therapies Targeting TAFs

TAFs as generic target in solid tumors

- Identification of specific marker of TAFs – fibroblast activation protein (FAP)
- Selection of specific cytotoxic T cells – streptamer-based
- Coculture of specific CTLs with TAFs
- Evaluation of cytotoxic potential of CTLs against TAFs - xCELLigence

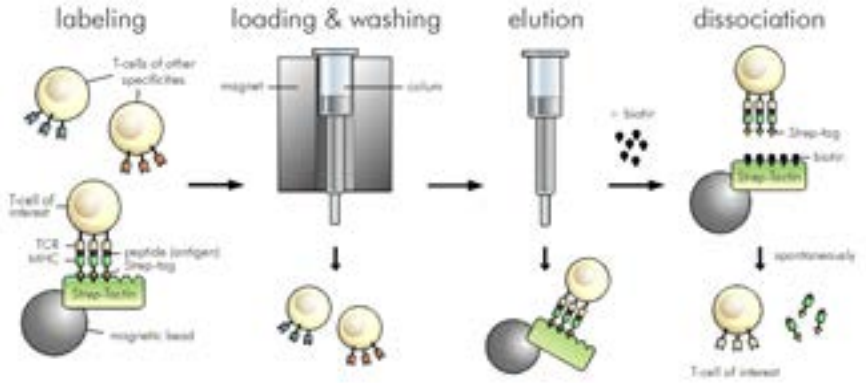

MHC I-Strep HLA-A*02:01
FAP 735-744, GLSGLSTNHL

```
  1 mktwvkivfg vatsavlall vmcivlrpsr vhnseentmr altlkdilng tfsyktffpn
 61 wisgqeylhq sadnnivlyn ietgqsytil snrtmksvna snyglspdrq fvylesdysk
121 lwrysytaty yiydlsngef vrgnelprpi qylcwspvgs klayvyqnni ylkqrpgdpp
181 fqitfngren kifngipdwv yeeemlatky alwwspngkf layaefndtd ipviaysyyg
241 deqyprtini pypkagaknp vvrifiidtt ypayvgpqev pvpamiassd yyfswltwvt
301 dervclqwlk rvqnvsvlsi cdfredwqtw dcpktqehie esrtgwaggf fvstpvfsyd
361 aisyykifsd kdgykhihyi kdtvenaiqi tsgkweaini frvtqdslfy ssnefeeypg
421 rrniyrisig syppskkcvt chlrkercqy ytasfsdyak yyalvcygpg ipistlhdgr
481 tdqeikilee nkelenalkn iqlpkeeikk levdeitlwy kmilppqfdr skkyplliqv
541 yggpcsqsvr svfavnwisy laskegmvia lvdgrgtafq gdkllyavyr klgvyevedq
601 itavrkfiem gfidekriai wgwsyggyvs slalasgtgl fkcgiavapv ssweyyasvy
661 terfmglptk ddnlehykns tvmaraeyfr nvdyllihgt addnvhfqns aqiakalvna
721 qvdfqamwys dqnhglsgls tnhlythmth flkqcfslsd
```

Streptamer enrichment of CTLs

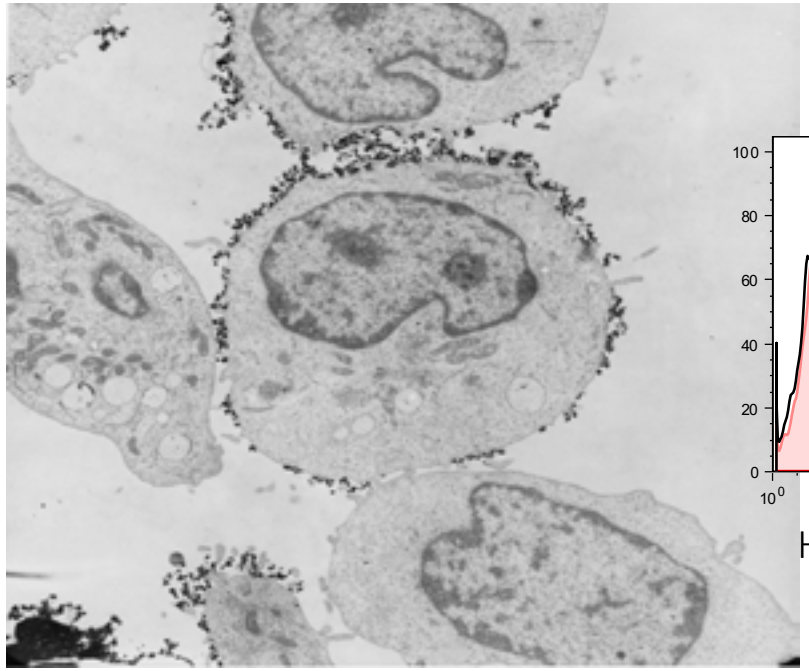

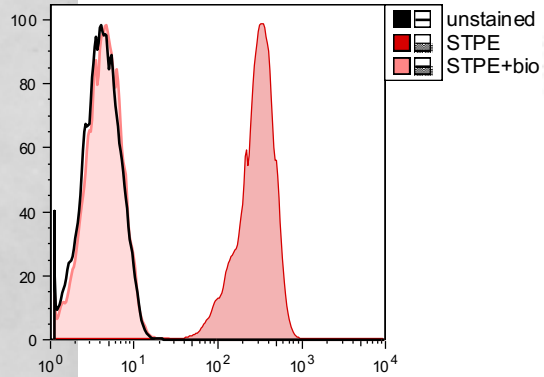

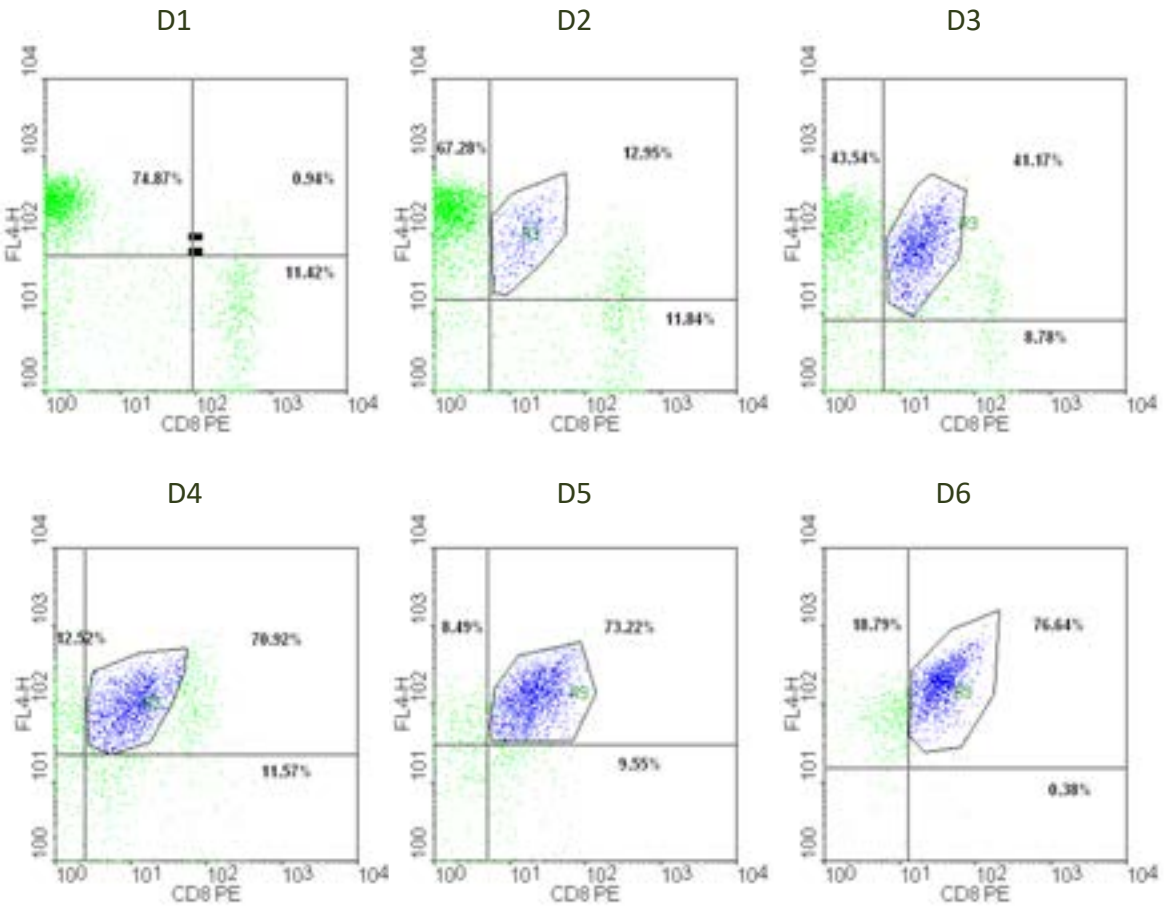

- FAP identified on TAF and custom-made MHC I-Strep HLA-A*0201 FAP for isolation of CD8+ specific T cells;
- Antigen-specific T cell sorting was performed by magnetic nanobeads separation, biotin-binding for removal of magnetic particles, and we performed co-culture of TAFs with positive and negative T cell fractions.

What is CAR and why we need CAR-T cells?

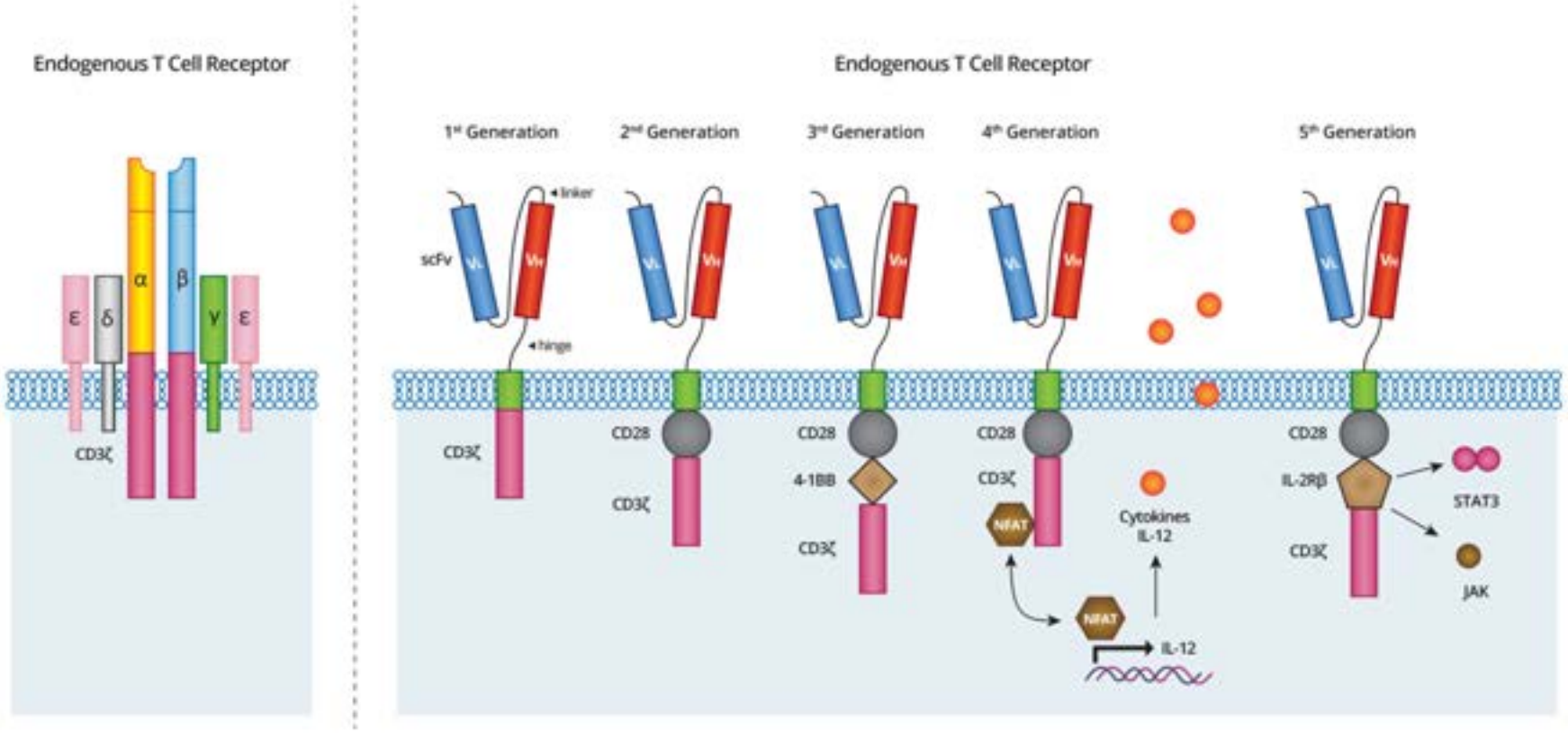

- Construction of Chimeric Antigen Receptor – CAR
- Selection of target antigen from the tumor microenvironment – FAP and Her2
- Construction of bispecific CAR targeting solid tumors

The bispecific anti-tumor CAR

Sequence 5' (restriction sequence BamHI, Kozak sequence)
CGGGATCCGCCACC
Signaling peptide (FcGR1B)
ATGTGGTTCTTGACAACTCTGCTCCTTTGGGTTCCAGTTGATGGG
scFv Sibrotuzumab, VH (8)
CAGGTACAGCTTGTGCAGTCCGGCGCTGAGGTCAAAAAACCAGGCGCCAGCGTTAAGGTGTCATGCAAGACTAGCAGGTATACATTCA
CTGAATACACAATACACTGGGTGCGACAGGCTCCCGGGCAAAGACTGGAGTGGATTGGGGGCATAAACCCCAACAATGGGATCCCGAA
TTATAATCAGAAATTTAAGGGTCGGGTGACAATCACAGTAGACACTAGCGCATCAACCGCCTACATGGAGCTCAGCTCCCTTAGGTCTGA
AGACACAGCAGTTTATTACTGCGCAAGGCGCCGCATCGCCTACGGCTATGACGAAGGTCATGCTATGGACTATTGGGGGCAAG
GGACACTCGTGACTGTCTCATCA
G4S Linker (2)
GGCGGCGGAGGAAGCGGAGGCGGAGGATCTGGGGGAGGCGGCTCTGGCGGAGGGGGATCT
scFv Sibrotuzumab, VL (9)
GACATTGTCATGACGCAGAGTCCTGACAGTCTCGCCGTGTCCTTGGGAGAGCGGGCAACAATCAATTGTAAAAGCAGCCAATCTCTCCT
GTACAGCCGGAACCAGAAGAACTACCTCGCCTGGTACCAGCAGAAACCCGGTCAGCCGCCCAAGCTCCTGATTTTTTGGGCCAGCACTC
GGGAAAGCGGTGTCCCCGACAGATTTTCCGGATCTGGCTTCGGGACAGATTTTACCCTGACGATCTCATCACTTCAGGCAGAGGATGTG
GCCGTCTACTACTGTCAACAGTATTTTTCCTACCCCCTCACTTTCGGCCAAGGAACCAAGGTGGAGATTAAA
Myc tag
GAGCAGAAGCTGATCTCCGAAGAGGACCTG
CD8a hinge (4)
GCCCTGAGCAACAGCATCATGTACTTCAGCCACTTCGTGCCCGTGTTTCTGCCCGCCAAGCCTACCACAACCCCTGCCCCTAGACCTCCTA
CCCCAGCCCCTACAATCGCCAGCCAGCCTCTGTCTCTGAGGCCCGAGGCTTCTAGACCTGCTGCTGGCGGAGCTGTGCATACCAGGGGC
CTGGAC
CD28 (5)
AAGCCCTTCTGGGTGCTGGTCGTGGTCGGCGGCGTGCTGGCCTGTTACAGCCTGCTGGTCACCGTGGCCTTCATCATCTTTTGGGTCCG
CAGCAAGAGAAGCCGGCTGCTGCACTCCGACTACATGAACATGACCCCCAGACGGCCTGGCCCCACCAGAAAGCACTACCAGCCCTAC
GCCCCTCCTAGAGATTTCGCCGCCTACCGGTCC
4-1BB (6)
AAACGGGGCAGAAAGAAACTCCTGTATATATTCAAACAACCATTTATGAGACCAGTACAAACTACTCAAGAGGAAGATGGCTGTAGCTG
CCGATTTCCAGAAGAAGAAGAAGGAGGATGTGAACTG
CD3z (7)
AGAGTGAAGTTCAGCAGGAGCGCAGACGCCCCCGCGTACCAGCAGGGCCAGAACCAGCTCTATAACGAGCTCAATCTAGGACGAAGAG
AGGAGTACGATGTTTTGGACAAGAGACGTGGCCGGGACCCTGAGATGGGGGGAAAGCCGAGAAGGAAGAACCCTCAGGAAGGCCTG
TACAATGAACTGCAGAAAGATAAGATGGCGGAGGCCTACAGTGAGATTGGGATGAAAGGCGAGCGCCGGAGGGGCAAGGGGCACGA
TGGCCTTTACCAGGGTCTCAGTACAGCCACCAAGGACACCTACGACGCCCTTCACATGCAGGCCCTGCCCCCTCGCTAA
scFv sequences of **Sibrotuzumab** were obtained from the US 2003/0103968 A1 Patent.

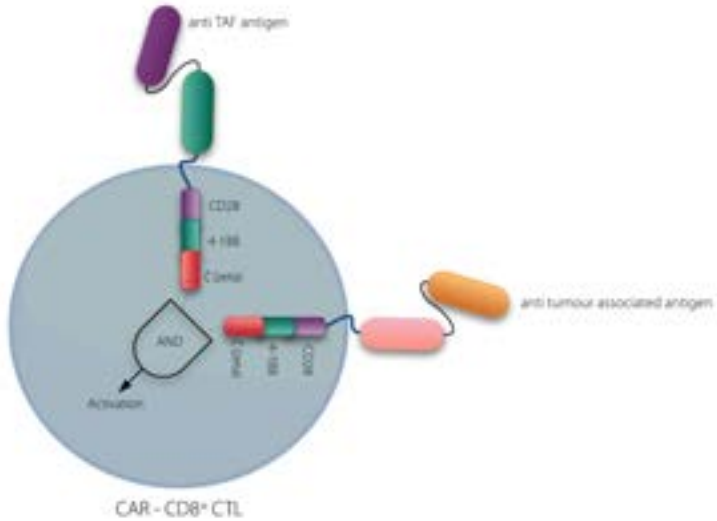

5'-3' sequences of anti-FAP CAR

The bispecific anti-tumor CAR

Sequence 5' (restriction sequence BamHI, Kozak sequence)
CGGGATCCGCCACC
Peptid semnal (FcGR1B)
ATGTGGTTCTTGACAACTCTGCTCCTTTGGGTTCCAGTTGATGGG
scFv Trastuzumab, VL (1)
GACATCCAGATGACCCAGAGCCCCAGCAGCCTGAGCGCCAGCGTGGGCGACAGGGTGACCATCACCTGCAGGGCCAGCCAGGACGTGAACACCGCCGTGGCCTGGTACCA
GCAGAAGCCCGGCAAGGCCCCCAAGCTGCTGATCTACAGCGCCAGCTTCCTGTACAGCGGCGTGCCCAGCAGGTTCAGCGGCAGCAGGAGCGGCACCGACTTCACCCTGAC
CATCAGCAGCCTGCAGCCCGAGGACTTCGCCACCTACTACTGCCAGCAGCACTACACCACCCCCCCCACCTTCGGCCAGGGCACCAAGGTGGAGATCAAGAGGACCGTGGCC
GCCCCCAGCGTGTTCATCTTCCCCCCCAGCGACGAGCAGCTGAAGAGCGGCACCGCCAGCGTGGTGTGCCTGCTGAACAACTTCTACCCCAGGGAGGCCAAGGTGCAGTGG
AAGGTGGACAACGCCCTGCAGAGCGGCAACAGCCAGGAGAGCGTGACCGAGCAGGACAGCAAGGACAGCACCTACAGCCTGAGCAGCACCCTGACCCTGAGCAAGGCCGA
CTACGAGAAGCACAAGGTGTACGCCTGCGAGGTGACCCACCAGGGCCTGAGCAGCCCCGTGACCAAGAGCTTCAACAGGGGCGAGTGC
G4S Linker (2)
GGCGGCGGAGGAAGCGGAGGCGGAGGATCTGGGGGAGGCGGCTCTGGCGGAGGGGGATCT
scFv Trastuzumab, VH (3)
GAGGTGCAGCTGGTGGAGAGCGGCGGCGGCCTGGTGCAGCCCGGCGGCAGCCTGAGGCTGAGCTGCGCCGCCAGCGGCTTCAACATCAAGGACACCTACATCCACTGGGT
GAGGCAGGCCCCCGGCAAGGGCCTGGAGTGGGTGGCCAGGATCTACCCCACCAACGGCTACACCAGGTACGCCGACAGCGTGAAGGGCAGGTTCACCATCAGCGCCGACA
CCAGCAAGAACACCGCCTACCTGCAGATGAACAGCCTGAGGGCCGAGGACACCGCCGTGTACTACTGCAGCAGGTGGGGCGGCGACGGCTTCTACGCCATGGACTACTGGG
GCCAGGGCACCCTGGTGACCGTGAGCAGCGCCAGCACCAAGGGCCCCAGCGTGTTCCCCCTGGCCCCCAGCAGCAAGAGCACCAGCGGCGGCACCGCCGCCCTGGGCTGC
CTGGTGAAGGACTACTTCCCCGAGCCCGTGACCGTGAGCTGGAACAGCGGCGCCCTGACCAGCGGCGTGCACACCTTCCCCGCCGTGCTGCAGAGCAGCGGCCTGTACAGC
CTGAGCAGCGTGGTGACCGTGCCCAGCAGCAGCCTGGGCACCCAGACCTACATCTGCAACGTGAACCACAAGCCCAGCAACACCAAGGTGGACAAGAAGGTGGAGCCC
Strep tag II (WSHPQFEK)
TGGAGCCACCCCCAGTTCGAGAAG
CD8a hinge (4)
GCCCTGAGCAACAGCATCATGTACTTCAGCCACTTCGTGCCCGTGTTTCTGCCCGCCAAGCCTACCACAACCCCTGCCCCTAGACCTCCTACCCCAGCCCCTACAATCGCCAGC
CAGCCTCTGTCTCTGAGGCCCGAGGCTTCTAGACCTGCTGCTGGCGGAGCTGTGCATACCAGGGGCCTGGAC
CD28 (5)
AAGCCCTTCTGGGTGCTGGTCGTGGTCGGCGGCGTGCTGGCCTGTTACAGCCTGCTGGTCACCGTGGCCTTCATCATCTTTTGGGTCCGCAGCAAGAGAAGCCGGCTGCTGC
ACTCCGACTACATGAACATGACCCCCAGACGGCCTGGCCCCACCAGAAAGCACTACCAGCCCTACGCCCCTCCTAGAGATTTCGCCGCCTACCGGTCC
4-1BB (6)
AAACGGGGCAGAAAGAAACTCCTGTATATATTCAAACAACCATTTATGAGACCAGTACAAACTACTCAAGAGGAAGATGGCTGTAGCTGCCGATTTCCAGAAGAAGAAGAAG
GAGGATGTGAACTG
CD3z (7)
AGAGTGAAGTTCAGCAGGAGCGCAGACGCCCCCGCGTACCAGCAGGGCCAGAACCAGCTCTATAACGAGCTCAATCTAGGACGAAGAGAGGAGTACGATGTTTTGGACAAG
AGACGTGGCCGGGACCCTGAGATGGGGGGAAAGCCGAGAAGGAAGAACCCTCAGGAAGGCCTGTACAATGAACTGCAGAAAGATAAGATGGCGGAGGCCTACAGTGAGA
TTGGGATGAAAGGCGAGCGCCGGAGGGGCAAGGGGCACGATGGCCTTTACCAGGGTCTCAGTACAGCCACCAAGGACACCTACGACGCCCTTCACATGCAGGCCCTGCCCC
CTCGCTAA

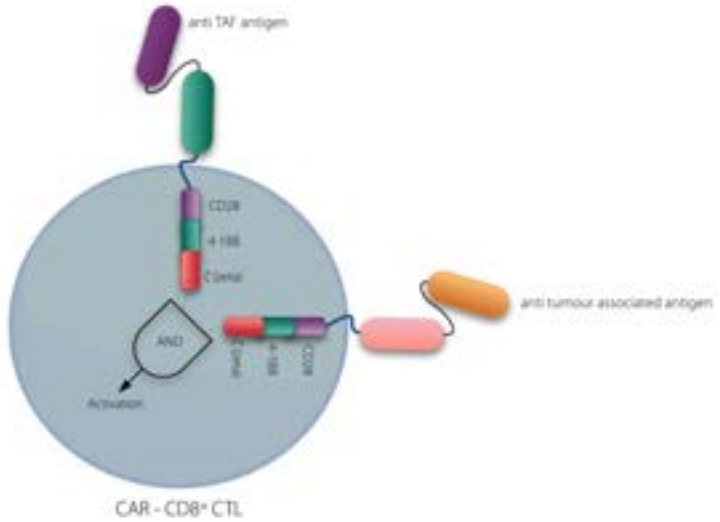

5'-3' sequences of anti-Her2 CAR

The bispecific anti-tumor CAR – How does it function?

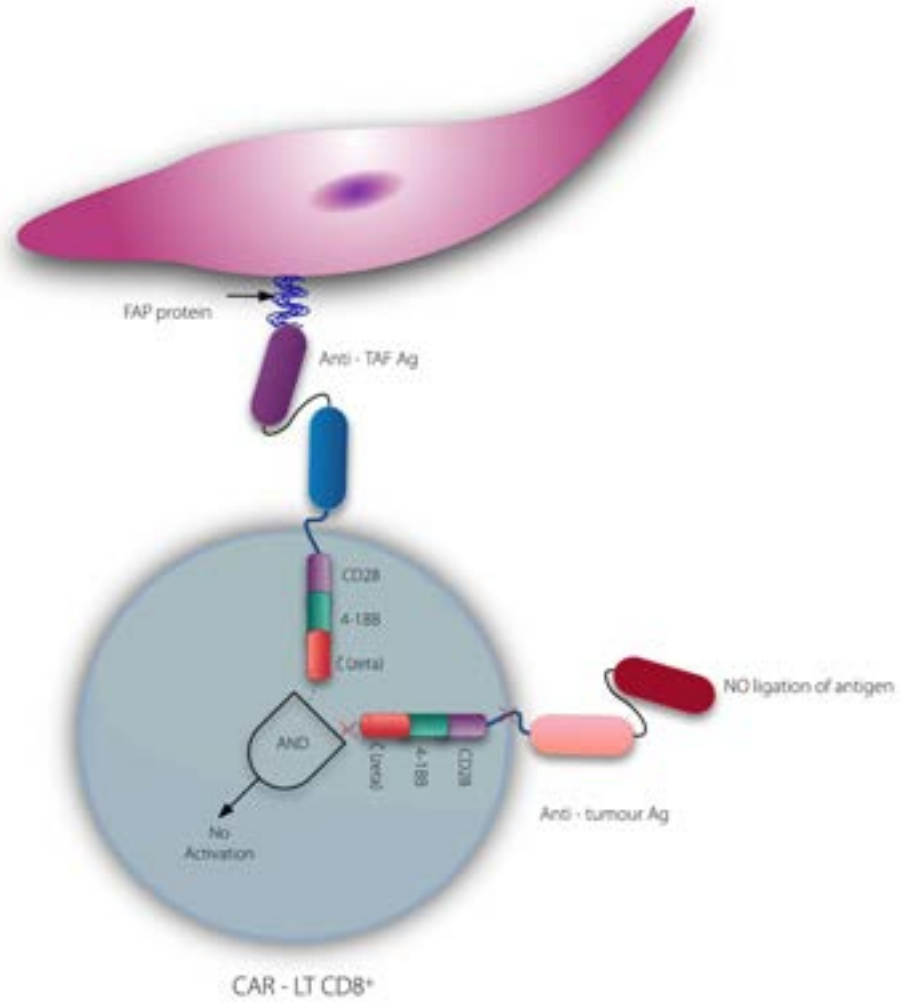

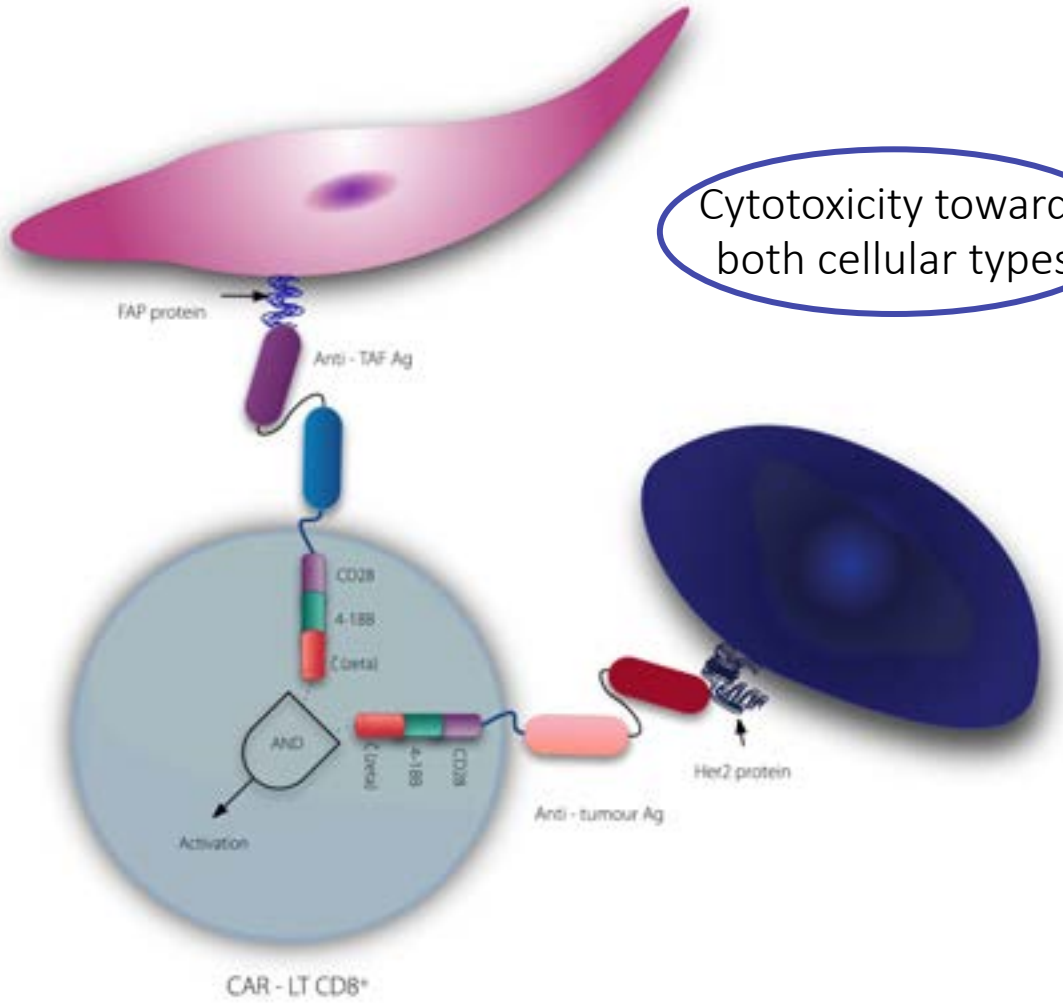

Cytotoxicity towards both cellular types

The bispecific anti-tumor CAR – Awards

- The present invention refers to construction of selective bispecific chimeric antigen receptor T cells (SMaRT CAR T cells) that target both tumor cells (TAA) and tumor microenvironment (TmAA);
- The generated CAR recognizes two TAAs and processes the signal in a true Boolean AND-gate fashion which requires the binding of both antigens in order to activate the T cell carrying the receptor;
- We will employ a trans-signaling strategy in which T-cell activation module of the CAR (CD3ζ) is physically dissociated from costimulatory signal (CD28)*

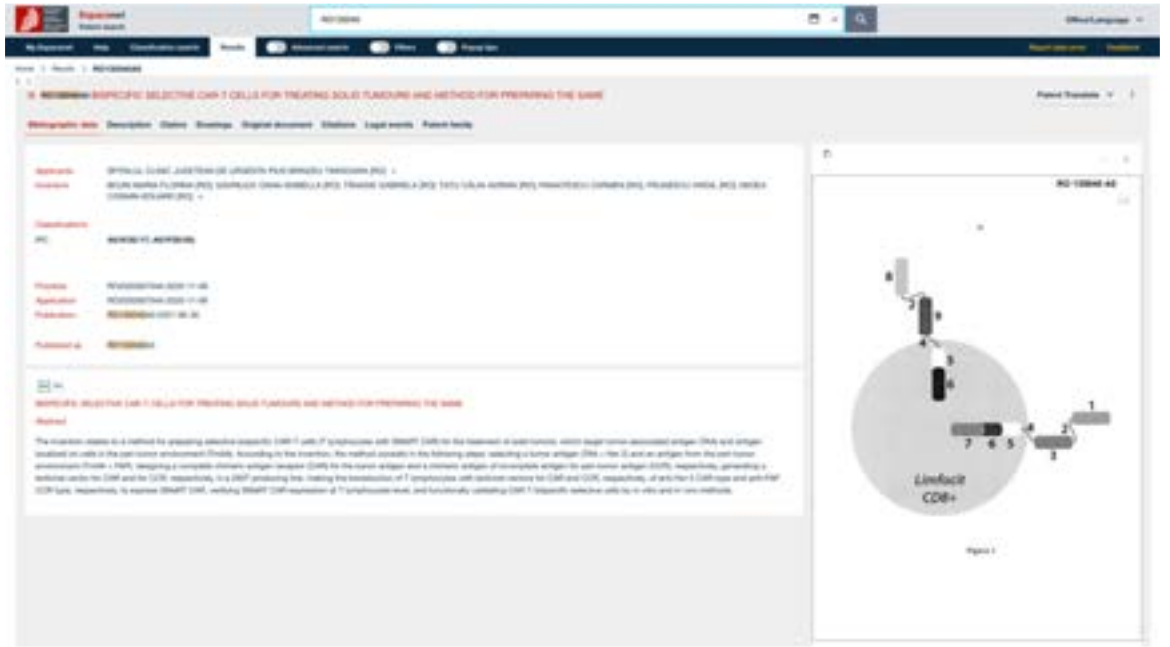

*Kloss CC, et al. *Nat Biotechnol.* 2013.

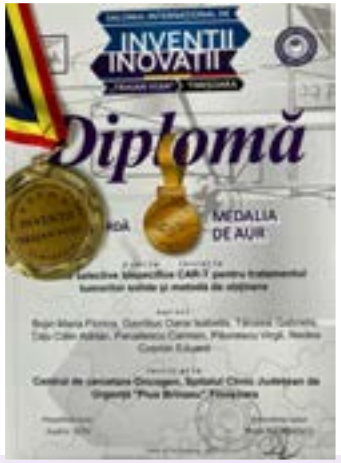

Bojin F, *et al.* Bispecific Selective CAR-T Cells for Treating Solid Tumors and the Method to Prepare Thereof. *OSIM Patent RO135040 (A0) – 2021-06-30*

Next generation sequencing (NGS) of tumor microenvironment with the purpose of novel therapeutic targets identification in solid tumors

Future perspectives

SMART DIASPORA 2023

Thank you!

Research team

Prof. Dr. Virgil Păunescu	Prof. Dr. Carmen Panaitescu
Prof. Dr. Carmen Tatu	Prof. Dr. Gabriela Tănasie
Conf. Dr. Călin Țațu	Prof. Dr. Adrian Neagu
Ș.L. Dr. Valentin Ordodi	Ș.L. Dr. Ivan Alexandra
As. Univ. Dr. Oana Gavriliuc	Ș.L. Dr. Nistor Daciana
Ș.L. Dr. Stelian Arjoca	As. Univ. Dr. Alexandru Tîrziu
Biol. Dr. Simona Anghel	Biol. Dr. Mirabela Cristea
Ing. Bioteh. Dr. Ada Telea	Biol. Dr. Elena Gai
Biol. Roxana Buzan	Chim. Dr. Alexandra Gruia
Biol. Manuela Grijincu	Biol. Lauriana Zbîrcea